

Epidemic extinction in a generalized susceptible-infected-susceptible model

Hanshuang Chen^{1,*}, Feng Huang², Haifeng Zhang^{3,†} and Guofeng Li¹

¹*School of Physics and Materials Science,
Anhui University, Hefei, 230601, China*

²*School of Mathematics and Physics,
Anhui Jianzhu University, Hefei 230601, China*

³*School of Mathematical Science, Anhui University, Hefei, 230601, China*

(Dated: November 30, 2016)

Abstract

We study the extinction of epidemics in a generalized susceptible-infected-susceptible model, where a susceptible individual becomes infected with the rate λ when contacting m infective individual(s) simultaneously, and an infected individual spontaneously recovers with the rate μ . By employing the Wentzel-Kramers-Brillouin approximation for the master equation, the problem is reduced to finding the zero-energy trajectories in an effective Hamiltonian system, and the mean extinction time $\langle T \rangle$ depends exponentially on the associated action \mathcal{S} and the size of the population N , $\langle T \rangle \sim \exp(N\mathcal{S})$. Because of qualitatively different bifurcation features for $m = 1$ and $m \geq 2$, we derive independently the expressions of \mathcal{S} as a function of the rescaled infection rate λ/μ . For the weak infection, \mathcal{S} scales to the distance to the bifurcation with an exponent 2 for $m = 1$ and 3/2 for $m \geq 2$. Finally, a rare-event simulation method is used to validate the theory.

PACS numbers:

*Electronic address: chenhsf@ahu.edu.cn

†Electronic address: haifengzhang1978@gmail.com

I. INTRODUCTION

The extinction of epidemics in finite populations is one of major challenges in population dynamics [1, 2]. Although many factors may contribute, such as environmental changes and social factors, intrinsic fluctuations, originated from discreteness of the reacting agents and the random character of their interactions, can induce a rare but large fluctuation along a most probable, or optimal, path to extinction of epidemics [3–5]. Unlike the fluctuation probability in equilibrium systems determined by the Boltzmann distribution, population dynamics is far away from equilibrium, and therefore, a general principle to determine the probability of large fluctuations in out-of-equilibrium system is still lacking.

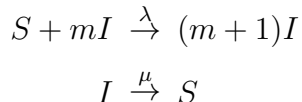
Many efforts have been done on this topic. Among them, many theoretical works have been focused on the calculation of mean extinct time (MET) of mathematical epidemic models, in which the systems possess a stable size of epidemic population which is metastable as rare large fluctuations always drive it to an absorbing state without infective individuals in finite populations. When the populations size is large, the Fokker-Planck approximation to the exact master equation that describes the stochastic process of the spreading only describes small deviations from the probability distribution maxima, but it fails to determine the probability of large fluctuations [6]. Elgart and Kamenev made an important progress in this topic, pioneered in Refs[7–10]: they employed the Peliti-Doi technique [11–14], to map the master equation into a Schrödinger-like equation that can identify the classical trajectory that connects the metastable fixed point and the absorbing state [15]. This allows them to calculate the classical action along this trajectory, a first approximation to the MET. Assaf and Meerson then suggested a general spectral method to improve the Elgart-Kamenev results [16, 17]. Kessler and Shnerb presented a general method to deal with the extinction problem based on the time-independent “real space” Wentzel-Kramers-Brillouin (WKB) approximation [18]. This method is easy to implement, its intuitive meaning is transparent, and its range of applicability covers any single species problem. These novel methods have been successfully applied to solve extinction problems in diverse situations, including time-varying environment [19, 20], catastrophic events [21], fragmented populations with migration [22, 23], complex networks [24, 25], and some others [26–31].

In this paper, we shall apply the WKB approximation to calculate the MET in a variant of susceptible-infected-susceptible (SIS) model, in which a susceptible individual becomes

infected with the rate λ when contacting m infective individual(s) simultaneously, and an infected individual spontaneously recovers with the rate μ . The population is well-mixed. For $m = 1$, the model recovers to the standard SIS model. $m \geq 2$ implies that a susceptible individual can be infected only if (s)he contacts at least two infective individuals. Since there are qualitatively different bifurcation features between $m = 1$ and $m \geq 2$, we calculate independently the MET, which is exponentially dependent on the action \mathcal{S} along the optimal extinction path and population size N . Near the infection threshold, we find that \mathcal{S} scales to the distance to the threshold with an exponent 2 for $m = 1$ and $3/2$ for $m \geq 2$. Lastly, we will use a rare-event simulation to validate the theoretical results.

II. MODEL

We consider a variant of the well-known SIS model. The model consists of N well-mixed individuals, in which each individual is either susceptible (S) or infected (I). The dynamics of the model is governed by the following reactions,



The first reaction describes that an individual S is infected when contacting at least m individuals I simultaneously with the infection rate λ , and the second one refers to the recovery process of an individual I with the recovery rate μ . Without loss of generality, we set $\mu = 1$. For a given integer m no less than one, the model is named as SIS m for convenience. For $m = 1$, the model recovers to the standard SIS model. For $m = 2$, the model has been studied on two-dimensional lattices [32, 33] and on complex networks [34, 35], which have found a discontinuous phase transition can emerge. A common feature for any m is that there always exists an absorbing state corresponding to not any more individuals I . This implies that the state cannot be left once the dynamics brings the system into it.

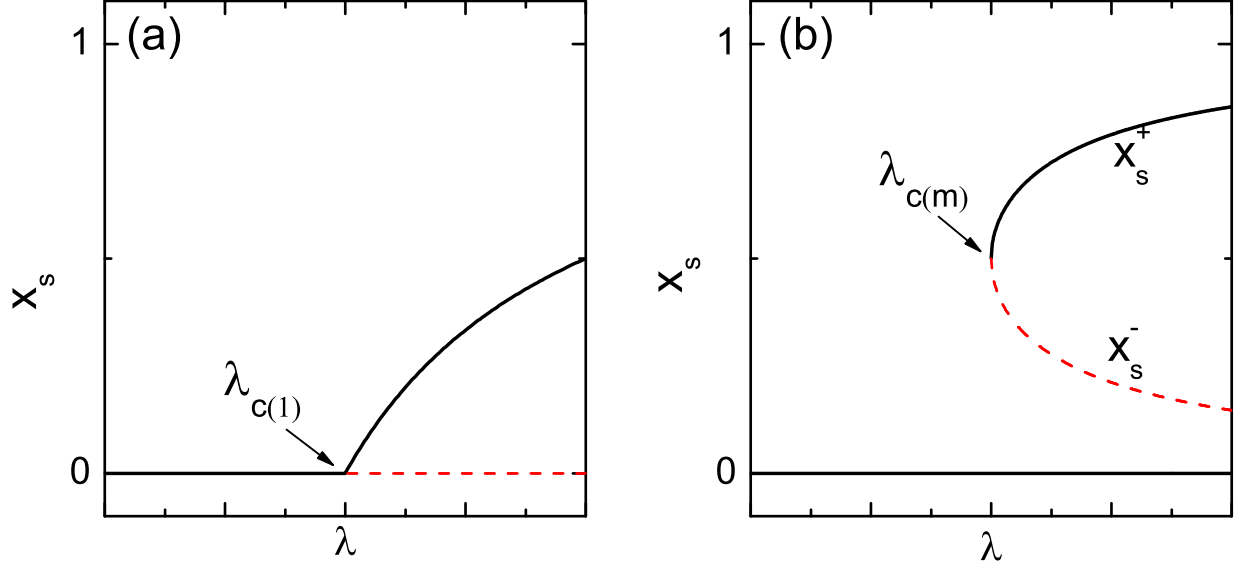


FIG. 1: (color online). Bifurcation diagrams of mean-field equation of x in the standard SIS model (a) and the SIS m ($m \geq 2$) model (b). The solid and dashed lines indicate the stable and unstable solution of x , respectively.

III. MEAN-FIELD THEORY

We proceed our analysis from the deterministic mean-field theory. The rate equation for the density x of individuals I can be written as

$$\dot{x} = \lambda(1 - x)x^m - x \quad (1)$$

where $x = n/N$ and n is the number of individuals I . It is clearly noticed that $x = 0$ is always a steady solution of Eq.1, corresponding to an epidemic-free state (absorbing state).

For the standard SIS model, it is well-known that the model undergoes a continuous phase transition from an epidemic-free state to an epidemic-spreading state at $\lambda = \lambda_{c(1)} \equiv 1$, as shown in Fig.1(a). For $\lambda < \lambda_{c(1)}$, the only stable steady solution of x is $x_s = 0$. For $\lambda > \lambda_{c(1)}$, the solution $x_s = 0$ becomes unstable and a new stable solution of epidemics emerges $x_s = 1 - \lambda_{c(1)}/\lambda$.

For the SIS m model with $m \geq 2$, we find that, by linear stability analysis, the solution $x_s = 0$ is always stable regardless of the value of λ , which is significantly different from the standard SIS model. Moreover, in order to seek nonvanishing solutions of x , it yields, by Eq.1, $x^{m-1}(1 - x) = 1/\lambda$, or equivalently, $y = 0$ where y is defined as $y = x^{m-1}(1 - x) - 1/\lambda$.

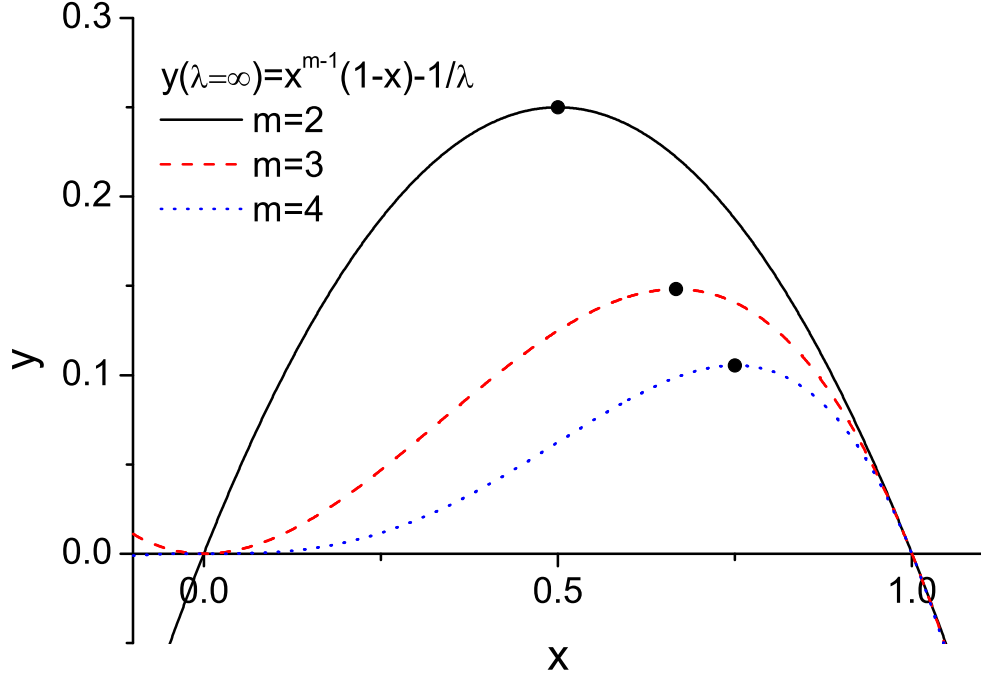


FIG. 2: (color online). $y = x^{m-1}(1-x) - 1/\lambda$ at $\lambda = \infty$ as a function of x for several m . The solid circles indicate the locations of the maxima in y for $x \in (0, 1)$

Firstly, in Fig.2 we plot y as a function of x at $\lambda = \infty$ ($1/\lambda = 0$) for several distinct values of m . Clearly, we find that y has a maximum $y_m = (m-1)^{m-1}/m^m$ at $x = x_m = (m-1)/m$. We then consider a finite $\lambda > 0$, in which the curves $y \sim x$ will be overall shifted downward with a quantity $1/\lambda$. If λ is large enough, the shift is so small that there exist two solutions of x between 0 and 1, denoted by x_s^\pm ($x_s^+ > x_s^-$). By linear stability analysis, one can easily check that x_s^+ is stable and x_s^- is unstable. If λ is decreased from above, the shift will become large enough until the two solutions vanish. At the critical case, $y_m = 1/\lambda$, leading to the critical value of λ for $m \geq 2$,

$$\lambda_{c(m)} = \frac{m^m}{(m-1)^{m-1}} \quad (m \geq 2) \quad (2)$$

The bifurcation diagrams for $m \geq 2$ are summarized in Fig.1(b). For $\lambda > \lambda_{c(m)}$, there are two stable solutions, $x_s = 0$ and $x_s = x_s^+$, and an unstable solution, $x_s = x_s^-$. Depending on the initial density of infected individuals, the model will arrive at either an epidemic-free state ($x_s = 0$) or an epidemic-spreading state ($x_s = x_s^+$). As λ decreases, x_s^+ and x_s^- get close to each other, until they colloid and annihilate at $\lambda = \lambda_{c(m)}$ via a saddle-node bifurcation.

For $\lambda < \lambda_{c(m)}$, the only stable solution is $x_s = 0$. Concretely, for the SIS2 model,

$$x_s^\pm = \frac{1}{2} \pm \frac{1}{2} \sqrt{\frac{\lambda - \lambda_{c(2)}}{\lambda}}, \quad \text{and} \quad \lambda_{c(2)} = 4 \quad (3)$$

For the SIS3 model,

$$x_s^\pm = \frac{1}{3} + \frac{1}{3} \cos \frac{\theta}{3} \pm \frac{\sqrt{3}}{3} \sin \frac{\theta}{3}, \quad \text{and} \quad \lambda_{c(3)} = \frac{27}{4} \quad (4)$$

where $\theta = \arccos(2\lambda_{c(3)}/\lambda - 1)$.

IV. MASTER EQUATION AND WKB APPROXIMATION

Since the mean-field treatment ignores the effect of stochastic fluctuations, it fails to account for the process of epidemic extinction induced by large fluctuations. To the end, let us define by $P_n(t)$ the probability that the number of infected individuals is n at time t . The master equation for $P_n(t)$ reads,

$$\frac{\partial P_n(t)}{\partial t} = W_+(n-1)P_{n-1}(t) + W_-(n+1)P_{n+1}(t) - [W_+(n) + W_-(n)]P_n(t) \quad (5)$$

where $W_+(n)$ ($W_-(n)$) is the infection (recovery) rate, given by

$$W_+(n) = \lambda(N-n) \prod_{l=0}^{m-1} \frac{n-l}{N} \quad (6)$$

and

$$W_-(n) = n \quad (7)$$

By employing the WKB approximation for the probability [3, 18], we write

$$P(n) = e^{-N\mathcal{S}(x)}. \quad (8)$$

As usual, we assume N is large and take the leading order in a N^{-1} expansion, by writing $P(n \pm 1) \approx P(n)e^{\mp \partial \mathcal{S} / \partial x}$ and $W(n \pm 1) \approx W(n)$. We can arrive at the Hamilton-Jacobi equation [3, 18],

$$\frac{\partial \mathcal{S}}{\partial t} + \mathcal{H}(x, p) = 0 \quad (9)$$

where \mathcal{S} and \mathcal{H} are called the action and Hamiltonian, respectively. As in classical mechanics, the Hamiltonian is a function of the coordinate x and its conjugate momentum $p = \partial\mathcal{S}/\partial x$,

$$\mathcal{H}(x, p) = w_+(x) (e^p - 1) + w_-(x) (e^{-p} - 1) \quad (10)$$

where $w_{\pm}(x) = W_{\pm}(n)/N$ are the reaction rates per person. Substituting Eq.6 and Eq.7 to Eq.10, we obtain

$$\mathcal{H}(x, p) = \lambda x^m (1 - x) (e^p - 1) + x (e^{-p} - 1) \quad (11)$$

We then write the canonical equations of motion,

$$\dot{x} = \partial_p \mathcal{H}(x, p) = \lambda x^m (1 - x) e^p - x e^{-p} \quad (12)$$

$$\dot{p} = -\partial_x \mathcal{H}(x, p) = -\lambda [m x^{m-1} - (m+1)x^m] (e^p - 1) - e^{-p} + 1 \quad (13)$$

We are interested in the extinction trajectory from an epidemic state to an extinct state of epidemics. This implies that there will be some trajectory along which \mathcal{S} is minimized, which represents the maximal probability of such an extinction event. This corresponds to the zero-energy ($\mathcal{H} = 0$) trajectory in the phase space (x, p) from an epidemic fixed point A to an extinction one C . According to Eq.11, the condition $\mathcal{H} = 0$ implies that there are three lines: $x = 0$, $p = 0$, and

$$\lambda x^m - \lambda x^{m-1} + e^{-p} = 0. \quad (14)$$

These three lines determine the topology of the optimal extinction path on the phase plane. Especially, the line $p = 0$ corresponds to the result of mean-field treatment, as Eq.12 for $p = 0$ recovers to the mean-field equation 1.

Fig.3(a) depicts the most probable trajectory of extinction in the standard SIS model from A to C via a fluctuational fixed point B . The coordinates on the phase space (x, p) of these points are: $A = (1 - \lambda_{c(1)}/\lambda, 0)$, $B = (0, -\ln \lambda)$, and $C = (0, 0)$. In general, the average time to reach extinction $\langle T \rangle$ is inversely proportional to the probability of the event, and thus can be related to our action by $\langle T \rangle \sim e^{N\mathcal{S}}$, where \mathcal{S} is given by

$$\mathcal{S}(m = 1) = \int p dx = \ln \lambda + \frac{1}{\lambda} - 1 \quad (15)$$

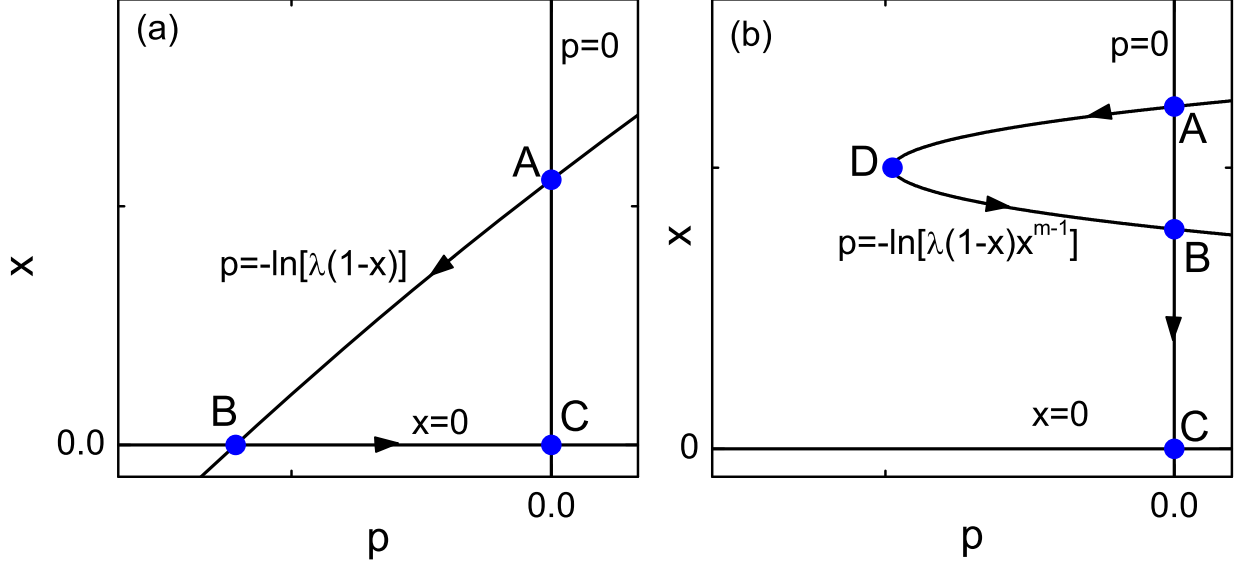


FIG. 3: (color online). The optimal path of extinction on the (x, p) plane for the standard SIS model (a) and the SIS_m ($m \geq 2$) model (b).

In Fig.3(b), we show the typical results for $m \geq 2$. The points A , B , and C locate at the mean-field line, and their coordinates (x, p) are: $A = (x_s^+, 0)$, $B = (x_s^-, 0)$, and $C = (0, 0)$. The action S can be analytically determined by

$$\mathcal{S}(m \geq 2) = \int_{x_s^-}^{x_s^+} \ln [\lambda x^{m-1} (1-x)] dx = F(x_s^+) - F(x_s^-) \quad (16)$$

with

$$F(x) = (\ln \lambda - m)x + (m-1)x \ln x - (1-x) \ln(1-x) \quad (17)$$

V. SCALING IN WEAK INFECTION REGIME

In the following, we will derive the scaling of the action \mathcal{S} with respect to the distance to the critical infection rate $\eta = \lambda - \lambda_c$ in the weak infection regime (i.e., $\eta \sim \mathcal{O}(1)$). For the standard SIS model close to $\lambda_{c(1)}$, the paths to extinction are approximately linear from A to B , and thus the action \mathcal{S} can be approximately calculated by [3, 36]

$$\mathcal{S}(m=1) \approx \frac{1}{2} \frac{\lambda - \lambda_{c(1)}}{\lambda} \ln \lambda \approx \frac{1}{2} \left(\frac{\lambda - \lambda_{c(1)}}{\lambda} \right)^2 \sim \eta^2 \quad (18)$$

For $m \geq 2$ and the infection rate close to $\lambda_{c(m)}$, the paths to extinction from A to B are approximately regarded as two lines connected by a point D , where $D = (x_m, -\ln(\lambda/\lambda_{c(m)}))$ corresponds to the peak of the curve described by Eq.14. Therefore, the action \mathcal{S} approximately equals to $\mathcal{S} \approx \frac{1}{2}(x_s^+ - x_s^-) \ln(\lambda/\lambda_{c(m)})$, where x_s^+ and x_s^- are the solutions of the equation $x^{m-1}(1-x) = 1/\lambda$. Since λ is close to $\lambda_{c(m)}$, the two solutions are very close to x_m , and thus we make an expansion $x_s^\pm = x_m \pm \epsilon$. Inserting the expansion to the above equation, we obtain $x_s^+ - x_s^- \approx 2\sqrt{(\lambda - \lambda_{c(m)})/\lambda\lambda_{c(m)}}$. Thus, we arrive at the scaling relation for $m \geq 2$,

$$\mathcal{S}(m \geq 2) \approx \sqrt{\frac{\lambda - \lambda_{c(m)}}{\lambda\lambda_{c(m)}}} \frac{\lambda - \lambda_{c(m)}}{\lambda_{c(m)}} \sim \eta^{\frac{3}{2}} \quad (19)$$

This is consistent with the standard scaling of the activation energy of escape near a saddle-node bifurcation point [10].

VI. NUMERICAL VALIDATION

In order to validate the theoretical results, we have made the stochastic simulation for the master equation (5) by Gillespie's algorithm [37, 38]. The main idea of Gillespie's algorithm is to randomly determine what the succeeding reaction step is and when it will happen according to the transition rates $W_\pm(n)$. However, epidemic extinction is a rare event that occurs very infrequently, especially for large λ or N . Thus, the conventional brute-force simulation becomes prohibitively inefficient. To overcome this difficulty, we have employed a recently developed rare-event sampling method, forward flux sampling (FFS) [39, 40], combined with Gillespie's algorithm. The FFS method first defines an order parameter to distinguish between the initial epidemic-spreading state \mathcal{I} and the final epidemic-free state \mathcal{F} , and then uses a series of interfaces to force the system from \mathcal{I} to \mathcal{F} in a ratchet-like manner. Here, it is convenient to select the number of infected individuals n as the order parameter. We define that the system is in \mathcal{I} if $n = n_0$ and it is in \mathcal{F} if $n = 0$, where $n_0 = Nx_s$ and x_s is the steady density of infected individuals at \mathcal{I} state. A series of nonintersecting interfaces n_i ($0 < i < N_{in}$) lie between states \mathcal{I} and \mathcal{F} , such that any path from \mathcal{I} to \mathcal{F} must cross each interface without reaching n_{i+1} before n_i , where N_{in} is the number of the interfaces. The algorithm first runs a long-time simulation which gives an estimate of the flux $\Phi_{\mathcal{I},0}$ escaping from the basin of \mathcal{I} and generates a collection of configurations corresponding to crossings

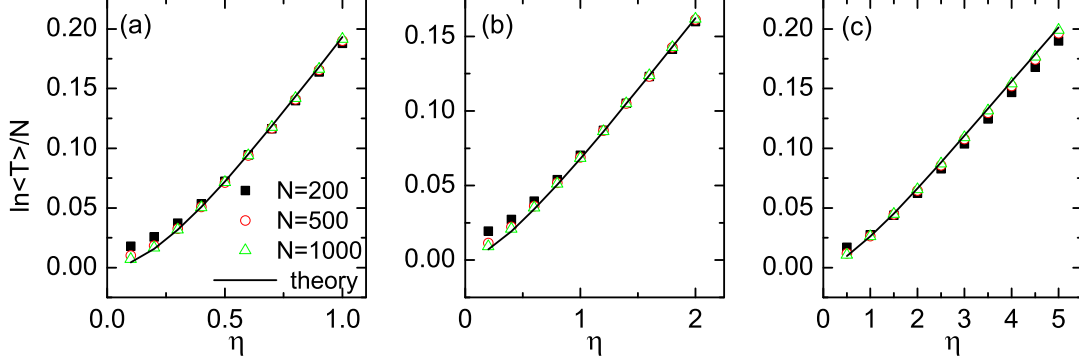


FIG. 4: (color online). $\ln\langle T \rangle/N$ as a function of $\eta = \lambda - \lambda_c(m)$ for $m = 1$ (a), $m = 2$ (b), and $m = 3$ (c). The lines indicate the theoretical results of the action \mathcal{S} from Eq.15 and Eq.16.

of the interface n_0 . The next step is to choose a configuration from this collection at random and use it to initiate a trial run which is continued until it either reaches n_1 or returns to n_0 . If n_1 is reached, store the configuration of the end point of the trial run. Repeat this step, each time choosing a random starting configuration from the collection at n_0 . The fraction of successful trial runs gives an estimate of the probability of reaching n_1 without going back into \mathcal{I} , $P(n_1|n_0)$. This process is repeated, step by step, until $n_{N_{in}}$ is reached, giving the probabilities $P(n_{i+1}|n_i)$ ($i = 1, \dots, N_{in} - 1$). Finally, we get the mean extinction time,

$$\langle T \rangle = \frac{1}{\Phi_{\mathcal{I},0} \prod_{i=0}^{N_{in}-1} P(n_{i+1}|n_i)} \quad (20)$$

In Fig.4(a-c), we show $\ln\langle T \rangle/N$ as a function of $\eta = \lambda - \lambda_c(m)$ for $m = 1, 2$, and 3 , respectively. Since $\langle T \rangle \sim e^{N\mathcal{S}}$, the action \mathcal{S} is comparable to $\ln\langle T \rangle/N$. For comparison, we plot the theoretical results of \mathcal{S} (Eq.15 and Eq.16), indicated by the lines in Fig.4. For large N , there are excellent agreements between the simulations and theoretical predictions for all λ . For small N , the agreements hold only for large λ . While for small N and λ , the theory disagrees the simulations. This is because that in this case $\langle T \rangle$ is not very long, such that $e^{N\mathcal{S}}$ can be comparable to its pre-exponential factor which was not considered in our analysis [41].

In the following, we shall show the numerical verification of the scaling relation near the bifurcation point. Along with Eq.18 and Eq.19, $\ln\langle T \rangle/N$ is expected to exhibit the scaling

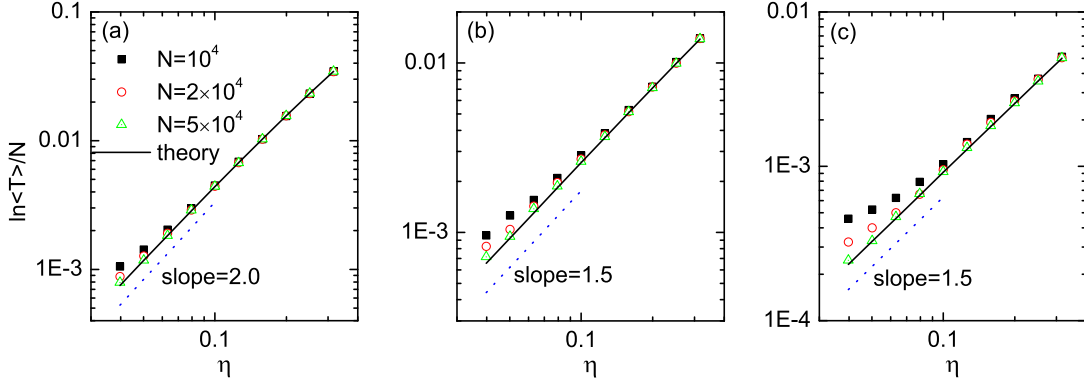


FIG. 5: (color online). Double logarithmic plot of $\ln\langle T \rangle/N$ as a function of $\eta = \lambda - \lambda_c(m)$ for $m = 1$ (a), $m = 2$ (b), and $m = 3$ (c). The solid lines indicate the theoretical results of the action \mathcal{S} from Eq.15 and Eq.16. The dotted lines indicate the reference slopes of the scaling near the epidemic thresholds from Eq.18 and Eq.19.

to η with an exponent 2 for $m = 1$ and $3/2$ for $m \geq 2$ near the epidemic threshold. Fig.5 shows $\ln\langle T \rangle/N$ as a function of η on double logarithmic coordinates for $m = 1, 2$, and 3 , respectively, in which we have used quite large N to reduce the contribution of the pre-exponential factor to $\langle T \rangle$. The simulation results agree well with the theoretical predictions from Eq.18 and Eq.19.

VII. CONCLUSIONS AND DISCUSSION

In conclusion, we have employed the WKB method to study the epidemic extinction process in a generalized SIS model (SIS m). The method transfers the master equation to an effective Hamilton system. This allows us to analytically determine the mean extinction time of epidemics, which is exponentially dependent on the population size N and the action \mathcal{S} along the zero-energy trajectories from the epidemic point to the extinction point on the phase space. Since the properties of bifurcation for $m = 1$ and $m \geq 2$ are different, we independently derive the analytical form of \mathcal{S} for the two cases. Near the epidemic bifurcation point, we obtain the scaling of \mathcal{S} with the distance to the bifurcation η , $\mathcal{S} \sim \eta^2$ for $m = 1$ and $\mathcal{S} \sim \eta^{3/2}$ for $m \geq 2$. Finally, we have used a rare-event simulation method,

FFS, to validate the theoretical results. While the model under study is a natural extension of the standard SIS model, a canonical model of epidemic spreading, it may be relevant to synergistic effects on the dynamics of opinion formation [42, 43]. If a group of neighboring persons to a selected person unanimously shares an opinion, the group pressure causes the selected person to take the opinion of the group. Therefore, the present theoretical study could provide useful understanding for the large fluctuation effect on the opinion dynamics. In the future, it would be desirable to consider the effect of interacting patterns among agents on the extinction of the generalized SIS model [24, 25].

Acknowledgments

This work was supported by National Science Foundation of China (Grants Nos. 11205002, 61473001, 11405001), the Key Scientific Research Fund of Anhui Provincial Education Department (Grant No. KJ2016A015) and “211” Project of Anhui University (Grant No. J01005106).

-
- [1] R. M. Anderson and R. M. May, *Infectious Diseases of Humans* (Oxford University Press, New York, 1991).
 - [2] J. R. Banavar and A. Maritan, *Nature* (London) **460**, 334 (2009).
 - [3] M. I. Dykman, I. B. Schwartz, and A. S. Landsman, *Phys. Rev. Lett.* **101**, 078101 (2008).
 - [4] M. Khasin and M. I. Dykman, *Phys. Rev. Lett.* **103**, 068101 (2009).
 - [5] A. Kamenev, B. Meerson, and B. Shklovskii, *Phys. Rev. Lett.* **101**, 268103 (2008).
 - [6] C. R. Doering, K. Sargsyan, and L. M. Sander, *Multiscale Model. Simul.* **3**, 283 (2005).
 - [7] R. Kubo, K. Matsuo, and K. Kitahara, *J. Stat. Phys.* **9**, 51 (1973).
 - [8] H. Gang, *Phys. Rev. A* **36**, 5782 (1987).
 - [9] C. S. Peters, M. Mangel, and R. F. Costantino, *Bull. Math. Biol.* **51**, 625 (1989).
 - [10] M. I. Dykman, E. Mori, J. Ross, and P. M. Hunt, *J. Chem. Phys.* **100**, 5735 (1994).
 - [11] M. Doi, *J. Phys. A* **9**, 1465 (1976).
 - [12] L. Peliti, *J. Phys. France* **46**, 1469 (1985).
 - [13] J. L. Cardy and U. C. Tauber, *Phys. Rev. Lett.* **77**, 4780 (1996).

- [14] J. L. Cardy and U. C. Tauber, J. Stat. Phys. **90**, 1 (1998).
- [15] V. Elgart and A. Kamenev, Phys. Rev. E **70**, 041106 (2004).
- [16] M. Assaf and B. Meerson, Phys. Rev. Lett. **97**, 200602 (2006).
- [17] M. Assaf and B. Meerson, Phys. Rev. E **75**, 031122 (2007).
- [18] D. A. Kessler and N. M. Shnerb, J. Stat. Phys. **127**, 861 (2007).
- [19] M. Assaf, A. Kamenev, and B. Meerson, Phys. Rev. E **78**, 041123 (2008).
- [20] M. Khasin, B. Meerson, and P. V. Sasorov, Phys. Rev. E **81**, 031126 (2010).
- [21] M. Assaf, A. Kamenev, and B. Meerson, Phys. Rev. E **79**, 011127 (2009).
- [22] M. Khasin, B. Meerson, E. Khain, and L. M. Sander, Phys. Rev. Lett. **109**, 138104 (2012).
- [23] M. Khasin, E. Khain, and L. M. Sander, Phys. Rev. Lett. **109**, 248102 (2012).
- [24] B. S. Lindley, L. B. Shaw, and I. B. Schwartz, EPL **108**, 58008 (2014).
- [25] J. Hindes and I. B. Schwartz, Phys. Rev. Lett. **117**, 028302 (2016).
- [26] A. Kamenev and B. Meerson, Phys. Rev. E **77**, 061107 (2008).
- [27] M. Khasin, M. I. Dykman, and B. Meerson, Phys. Rev. E **81**, 051925 (2010).
- [28] B. Meerson and P. V. Sasorov, Phys. Rev. E **83**, 011129 (2011).
- [29] O. Gottesman and B. Meerson, Phys. Rev. E **85**, 021140 (2012).
- [30] E. Y. Levine and B. Meerson, Phys. Rev. E **87**, 032127 (2013).
- [31] N. R. Smith and B. Meerson, Phys. Rev. E **93**, 032109 (2016).
- [32] D.-J. Liu, X. Guo, and J. W. Evans, Phys. Rev. Lett. **98**, 050601 (2007).
- [33] D.-J. Liu, J. Stat. Phys. **135**, 77 (2009).
- [34] C. Varghese and R. Durrett, Phys. Rev. E **87**, 062819 (2013).
- [35] H. Chae, S.-H. Yook, and Y. Kim, New J. Phys. **17**, 023039 (2015).
- [36] I. B. Schwartz, L. Billings, M. Dykman, and A. Landsman, J. Stat. Mech. **01**, P01005 (2009).
- [37] D. T. Gillespie, J. Comp. Phys. **22**, 403 (1976).
- [38] D. T. Gillespie, J. Phys. Chem. **81**, 2340 (1977).
- [39] R. J. Allen, P. B. Warren, and P. R. ten Wolde, Phys. Rev. Lett. **94**, 018104 (2005).
- [40] R. J. Allen, C. Valeriani, and P. R. ten Wolde, J. Phys.: Condens. Matter **21**, 463102 (2009).
- [41] M. Assaf and B. Meerson, Phys. Rev. E **81**, 021116 (2010).
- [42] F. J. Pérez-Reche, J. J. Ludlam, S. N. Taraskin, and C. A. Gilligan, Phys. Rev. Lett. **106**, 218701 (2011).
- [43] D. Centola, Science **329**, 1194 (2010).